Journal of Physics A: Mathematical and Theoretical

PAPER

Filling space with polydisperse spheres in a non-Apollonian way

To cite this article: Robert Botet *et al* 2021 *J. Phys. A: Math. Theor.* **54** 195201

IOP Publishing Journal of Physics A: Mathematical and Theoretical

J. Phys. A: Math. Theor. **54** (2021) 195201 (18pp) https://doi.org/10.1088/1751-8121/abef81

Filling space with polydisperse spheres in a non-Apollonian way

Robert Botet[1,*], **Sylvie Kwok**[2] and **Bernard Cabane**[2]

[1] Laboratoire de Physique des Solides Bât. 510, CNRS UMR8502, Université Paris-Saclay, Centre d'Orsay, F-91405 Orsay, France

[2] CBI, ESPCI, CNRS, PSL University, 75005 Paris, France

E-mail: robert.botet@universite-paris-saclay.fr

Received 19 January 2021, revised 10 March 2021
Accepted for publication 17 March 2021
Published 16 April 2021

Abstract

Completing a Swiss-cheese theorem of Lieb and Lebowitz (LL), we prove that any population of spheres with power-law radius distribution $\propto 1/r^{d_{\mathrm{f}}+1}$ can completely fill 3D Euclidean space if the exponent is such that $2.8 \leqslant d_{\mathrm{f}} < 3$. This sufficient condition extends considerably the known part of the ensemble of space-filling populations of polydisperse spheres. The self-similar spatial arrangement of the polydisperse spheres related to the theorem is discussed using a numerical example with $d_{\mathrm{f}} = 2.875$. By calculating the small-angle scattering structure factor of the resulting packing, we found it to present several crystalline peaks indicating some regularity. This is significantly different from the featureless structure factor of an Apollonian packing which represents total disorder. We thereby argue that the LL algorithm for filling space with spheres is fundamentally different from Apollonian constructions.

Keywords: dense sphere packing, Apollonian sphere packing, fractal interface

(Some figures may appear in colour only in the online journal)

1. Introduction

Dense vitreous materials are much sought after because of their unique technological applications. Indeed, they manifest remarkable mechanical properties such as high resilience and high formability [1]; they often possess amazing optical and electrical properties [2]; their thermal properties are anomalous [3] etc. Two classic examples of dense vitreous materials are (1) vitrified ceramics [4] and (2) ultra-high performance concrete [5]. A main issue for the practical preparation of such materials is that the disordered local structure requires a lot of energy (thermal and mechanical) to obtain and control [6]. Therefore, any avenue to lower energy consumption is of paramount interest. An efficient way to get around the problem is to

[*] Author to whom any correspondence should be addressed.

pack together a large population of small particles to form a paste as dense as possible before melting or sintering the paste to eliminate tiny voids and obtain the final vitreous material [7]. Intuitively, it is clear that such an approach requires a very wide initial size distribution since one has to use smaller and smaller pieces to occupy the likewise increasingly smaller voids remaining in the packed system during the filling process. Hence the crucial question: is there an optimal particle size distribution that can give the most compact paste by simple mixing?

We address here this question when the particles are all spherical in shape, because spherical particles are either natural in some cases (e.g. extremely dense emulsions of spherical droplets may result from elastic energy minimization [8]), or provide good approximation for small pebbles or convex grains. In spite of Ulam's packing conjecture [9] stating that spheres are one of the worst possible cases of all the convex bodies for occupying space densely [10, 11], the number of space-filling populations of spheres is nonetheless expected to be very limited and thus relatively easy to identify. From the current state of the art, we know that polydisperse sphere populations with power-law distributions, $n(r) \propto 1/r^{d_\mathrm{f}+1}$, of the sphere radii r, can geometrically fill space entirely without overlaps when the exponent d_f has specific values: $d_\mathrm{f} \simeq 2.47$ (numerical result) [12], $d_\mathrm{f} \simeq 2.73$ (numerical result) [13], any value of d_f such that $2.47 < d_\mathrm{f} < 2.88$ (numerical range) [14] and an infinite number of discrete values of d_f between 2.9885 and 3 (exact result) [15].

Interestingly, the last result, engendered by a little-known theorem of Lieb and Lebowitz (LL) [15], is often neglected in modern discussions pertaining to dense sphere-packings. A brief literature search in the domain reveals a multitude of publications relating to Apollonian packing algorithms, but few mentions of the LL algorithm (likely due to its description having been casually tucked away by the authors within a dense mathematical work). In the present work, we seek to revive general interest in the LL theorem, by extending it to demonstrate that any population of spheres with $2.8 \leqslant d_\mathrm{f} < 3$ (exact range) can be packed as densely as desired without overlaps. In fact, several naturally-occurring distributions are empirically known to be within these bounds, e.g. (see [16] for extensive data) gravel ($d_\mathrm{f} \simeq 2.82$) or glacial tills ($d_\mathrm{f} \simeq 2.88$). We compare LL and Apollonian packings in the 3D space, deducing that the extended LL theorem authorises space-filling populations of spheres previously inaccessible by Apollonian constructions.

Our initial motivation was to compare packings resulting from the LL algorithm and packings found in our own experiments of extremely dense emulsions of spherical droplets [8, 17] that we had established were Apollonian in nature. We then discuss in the present work sphere arrangements in only the 3D Euclidean space. Similar work could also be interesting to perform in the 2D space, though it may be challenging to obtain experimental physical results in the 2D space for comparison.

1.1. The mathematical context

The enduring popularity of Apollonian constructions has a historical root. From the mathematical point of view, Leibniz [18] was the first to propose an algorithm to cover the 2D Euclidean space with an infinite number of disks of decreasing radii, based on a geometric construction introduced by Apollonius de Perga that builds a disk tangent to three existing disks. Much later, Mandelbrot [19] conjectured that one could use a similar algorithm to fill the 3D Euclidean space with spheres arranged in a self-similar way. A rigorous self-similar packing algorithm based on inversive geometry was proposed in [14]. All Apollonian algorithms are based on a maximal geometric condition and is generically called 'osculatory packing' [12] or 'Apollonian packing' [20]. In 3D, it is based on the iterative addition of the largest interstitial sphere compatible (that is without overlaps) with the biggest void remaining in the system [21].

The algorithm can be used to build regular and disordered packings alike, attaining the final volume fraction $\phi = 1$ [22] (in the mathematical sense, the interior of the set complementary to the sphere packing is of null measure).

An osculatory packing definitely different from Apollonian has been suggested by Manna in [23]. In the Apollonian algorithm, the nth sphere is the largest sphere consistent with the empty pore space left by the $n - 1$ spheres, whereas in Manna's algorithm, the centre of the nth sphere is chosen randomly in the empty pore space of the $n - 1$ spheres and its radius is the largest possible in that place. Manna's algorithm is also known as a packing-limited growth, i.e. the growth of the nth sphere is limited by others already in the packing. Both algorithms are in the group of the 'osculatory algorithms' since the nth sphere is tangent to at least one of the $n - 1$ spheres, but the Apollonian algorithm is known to require significantly fewer small spheres than Manna's case.

1.2. The self-similar assumption

In the following, we consider the problem of totally filling a unit cube with a polydisperse population of perfect spheres.

By firstly packing spheres all of the same radius, one can obtain a system of maximum volume fraction $\phi = \pi/3\sqrt{2} \simeq 0.74$ if the arrangement is regular (face-centered cubic lattice), or $\phi \simeq 0.64$ if the packing is disordered (random close packing) [24]. The next step is to fill with smaller spheres the voids remaining in the system. Using again monodisperse spheres of radius smaller than the radius of the largest void insphere, one can increase the volume fraction of the system. But because of their complicated shapes, one cannot totally fill the voids in such a way: when this second step is completed, many smaller voids still remain. These voids can be partially filled in the same manner; by iterating the process using increasingly smaller spheres, all voids are eventually filled completely when the sphere radius tends to 0. Note that such schematic description of this algorithm does not require any length scale to be defined, and one can then expect the resulting packing to be self-similar. Therefore, we are now looking for a radius distribution of the spheres, $n(r)$, in the form of a scale-free power law [25, 26]:

$$n(r) \propto \frac{1}{r^{d_\mathrm{f}+1}}. \tag{1}$$

The radius distribution is written here as a continuous distribution of the radii, r, but discrete distribution can be used as well (and will be used later on). The exponent, d_f, of the power law is a positive constant equal to the fractal dimension of the matter-void interface [27, 28], that is, asymptotically, the union of the surfaces of all the spheres forming the packing [23].

1.3. The fractal dimensions of the Apollonian packing and related sphere packings

The value, $d_\mathrm{f}^\mathrm{Apo}$, of the fractal dimension of the 3D Apollonian packing has been variously and precisely estimated from intensive numerical works [12, 21]:

$$d_\mathrm{f}^\mathrm{Apo} = 2.4739\ldots. \tag{2}$$

It would appear that the value (2) is characteristic of an osculatory packing process as it is the same whether the initial packing is regular or random. Slightly different values of d_f have also been found for non-osculatory, packing-limited growth algorithms. [13, 29].

Besides the commonly discussed Apollonian packing, Lieb and Lebowitz [15] also described filling space with populations of spheres whose radii are power-law distributed as long as the corresponding value of d_f is larger than 2.9885. In the following sections, we examine how the original LL theorem may be extended down to $d_\mathrm{f} = 2.8$, by gradually approaching a spherical geometry from known space-filling polyhedra (known as plesiohedra).

1.4. Wesler's theorem

A theorem by Wesler [30] states that the total surface of any sphere-packing filling the unit cube is infinite. Then, applying the theorem to the radius-distribution (1), the value of d_f must be in the range:

$$2 \leqslant d_\mathrm{f} < 3. \tag{3}$$

This condition was tentatively improved upon by Aste [26], who argued that among all the space-filling polydisperse sphere packings, the Apollonian packing is the one with the lowest possible value of d_f (i.e. with the smallest proportion of tiny spheres). Then, a necessary condition stronger than (3) for spheres filling space could be: $2.4739 \leqslant d_\mathrm{f} < 3$; up to now, this argument remains a conjecture.

In the following, we demonstrate and discuss *sufficient* conditions of the form (3) on the value of d_f for a population of spheres with radius distribution (1) to be space-filling. As the argument uses space-filling polyhedra, we start first in setting out a short review of these objects.

2. Space-filling polyhedra

2.1. Definitions of two geometric quantities related to convex bodies

Let us call $\omega(r)$ a finite convex body, in which r is the radius of the insphere, that is the largest sphere that can fit inside $\omega(r)$ [31]. We introduce two characteristic numbers related to $\omega(r)$:

- the asphericity number [11] γ_c is the ratio between the radius of the circumscribed sphere (that is the smallest sphere containing $\omega(r)$) and the radius of the insphere. The index $_\mathrm{c}$, in 'γ_c', is to remind that this number is related to the circumscribing sphere
- the number α_v comes from the volume of $\omega(r)$, written: $\alpha_\mathrm{v} 4\pi r^3/3$. The index $_\mathrm{v}$, in 'α_v', reminds one that this number is related to the volume of the convex body

These characteristic numbers are practical for measuring the distances in terms of r for the convex body $\omega(r)$.

Note that if $\omega(r)$ is the sphere of radius r, these quantities are respectively: $\gamma_\mathrm{c} = 1$, $\alpha_\mathrm{v} = 1$.

2.2. Introducing the plesiohedra

Perfect tessellation of space with identical polyhedra has been a long-pondered problem. An anecdote attributed to Aristotle (4th century BC) is well known: he proclaimed without proof in his book *De Caelo* that space could be filled by identical tetrahedra ['*among solids* (*it is agreed that*) *only two* (*fill the place that contain them*), *the regular tetrahedron and the cube*']. This conjecture was disproved in the 15th century by Regiomontanus in a lost manuscript [32, 33]. Even back then, it was already recognized that drawing up a complete list of space-filling polyhedra was not as straightforward a problem as one would have thought.

Many different convex polyhedra have been found to fill 3D Euclidean space by tiling identical copies of them. They are generically named plesiohedra [34]. We shall restrict the following discussion to three convex plesiohedra selected among the five parallelohedra, because they are simple and rather 'close' to the sphere (figure 1). We list these selected plesiohedra in decreasing order of γ_c (smaller γ_c corresponds to more sphere-like polyhedra):

- the cube is the only Platonic solid to be a plesiohedron. Its characteristics are: $\gamma_c = \sqrt{3} \simeq 1.73$ and $\alpha_v = 6/\pi \simeq 1.90$. The Cartesian coordinates of the 8 vertices of the cube $\omega(r)$ centred at the origin $(0, 0, 0)$ are: $(\pm r, \pm r, \pm r)$. The cube is the Wigner–Seitz cell of the regular simple cubic lattice.
- The rhombic dodecahedron is an Archimedean solid that has: $\gamma_c = \sqrt{2} \simeq 1.41$ and $a_v = \sqrt{18}/\pi \simeq 1.35$. The Cartesian coordinates of the 14 vertices of the rhombic dodecahedron $\omega(r)$ centred at the origin are: $(\pm r/\sqrt{2}, \pm r/\sqrt{2}, \pm r/\sqrt{2})$, $(\pm r\sqrt{2}, 0, 0)$, $(0, \pm r\sqrt{2}, 0)$ and $(0, 0, \pm r\sqrt{2})$. The rhombic dodecahedron is the Wigner-Seitz cell of the regular fcc lattice.
- The Kelvin's truncated octahedron is another space-filling Archimedean solid that has: $\gamma_c = \sqrt{5/3} \simeq 1.29$ and $a_v = 8/\pi\sqrt{3} \simeq 1.47$. The Cartesian coordinates of the 24 vertices of the truncated octahedron $\omega(r)$ centred at the origin are: $(0, \pm r/\sqrt{3}, \pm 2r/\sqrt{3})$ and the six permutations of the three coordinates. The truncated octahedron is the Wigner–Seitz cell of the regular bcc lattice.

3. General sufficient space-filling conditions

Let us consider the ensemble whose elements are all the populations of perfect spheres with discrete distribution of their radii, r_k, such that:

$$\{n_k, r_k\}_{k=0,1,2,\ldots} \text{ means } n_k \text{ spheres } (n_k \in \mathbb{N}^\star) \text{ of radius } r_k, \tag{4}$$

$$k \to r_k \text{ is a decreasing sequence of positive real numbers },$$

$$n_k r_k^3 \leqslant \frac{1}{\sqrt{32}} \text{ for any } \quad k = 0, 1, 2, \ldots \tag{5}$$

$$\sum_{k=0}^{\infty} n_k r_k^3 = \frac{3}{4\pi} \text{ (space-filling condition of the packing)}, \tag{6}$$

$$\sum_{k=0}^{\infty} n_k r_k^2 = \infty \quad \text{(infinite surface of the packing)}. \tag{7}$$

For every population in the ensemble above, the index k is called the rank. The condition (5) expresses that the ensemble of monodisperse spheres of rank k cannot constitute a volume fraction larger than the maximum value $\pi/3\sqrt{2}$.

Though necessary for spheres with discrete radius distribution, (5)–(7) do not constitute sufficient conditions to represent a space-filling population of spheres. To do so, one has to find a geometrical algorithm able to build iteratively the sphere-packing into the unit cube, adding n_k spheres of radius r_k without overlap at each rank k. This way is analogous to invoking a kind of Maxwell's demon able to put each sphere at its correct place in space [35].

3.1. Sufficient condition using the LL algorithm

The following algorithm—named 'LL algorithm' since it was introduced by Lieb and Lebowitz in [15]—can be used to build perfect packing of spheres complying with (5)–(7). We describe below the algorithm starting from the 3D cube of edge length 1, though any initial 3D compact

Figure 1. Sketch of the three plesiohedra used as examples in this work. From left to right: the cube, the rhombic dodecahedron and the truncated octahedron. The respective circumscribing spheres show how 'round' these plesiohedra are.

domain can, in principle, be used (in [15], the unit ball was used instead). In the case of the unit cube, the unit length is defined as the cube edge, i.e. all particle radii in the formulae below will be expressed on the scale of the cube-edge length.

3.2. Running through the LL algorithm

At rank 0 of the sphere packing, n_0 spheres of radius r_0 are placed without overlap inside the empty cube of edge length 1 (periodic boundary conditions are used). Placement of these spheres can be regular or random, and they act as seeds for the packing. Such placement is possible because of (5). When the rank 0 is completed, the volume V_0 of the domain Ω_0 left empty in the cube is:

$$V_0 = 1 - \frac{4\pi}{3} n_0 r_0^3 < 1. \tag{8}$$

In the LL algorithm, a loop of iteration builds the system of rank j from the system completed at rank $j-1$, that is when all the n_k spheres of radius r_k, $k = 0, 1, \ldots, j-1$, have been positioned inside the cube by the Maxwell's demon. The main loop is as follows:

- loop '$j-1 \rightarrow j$':
  - Step 1: part of the empty domain Ω_{j-1} is covered with a dense regular array of ν_j non-overlapping identical plesiohedra $\omega(r_j)$, each of them totally included inside Ω_{j-1} (that is none of these polyhedra intersects the boundaries of Ω_{j-1}). This step can always be completed as long as the value of of r_j is so small that $\nu_j \geqslant 1$.
  - Step 2: n_j plesiohedra are chosen amongst the ν_j, and replaced by their inspheres. The selection of the plesiohedra is random. The value of n_j is given by (4). The $\nu_j - n_j$ remaining polyhedra are left empty. Clearly, this step can be achieved provided $n_j \leqslant \nu_j$.

After the loop has been completed, it results in the void Ω_{j-1} of volume

$$V_{j-1} = 1 - \frac{4\pi}{3} \sum_{k=0}^{j-1} n_k r_k^3 < 1, \tag{9}$$

in the system.

The loop above starts from $j = 1$, and is continued for all positive integerinteger positive values of j. The radii r_k being all > 0, the sequence of void volumes V_{j-1}, as written in (9),

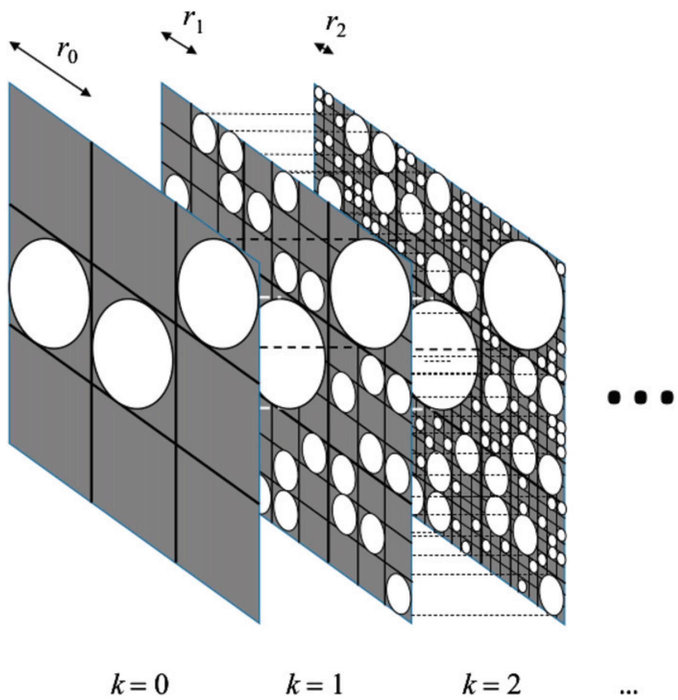

Figure 2. The 2D LL algorithm in the unit square, described as a Swiss-cheese model. At rank $k = 0$, an initial tessellation with big squares is used and the initial holes are the open disks inscribed in n_0 squares. These initial circular holes are kept at rank $k = 1$. Then, n_1 smaller squares of edge length r_1 are created to tile the plane, wherein open disks are randomly inscribed so long as they do not intersect with any other holes. At rank $k = 2$, smaller tiling squares of edge length r_2 are used in which newer open disks are now inscribed without overlaps with all existing holes, etc. In this manner, the iteration is performed such that the plane at rank k is punched by a number of non-overlapping open disks, and, for $k \to \infty$, the unit square is full except for the complementary set of the union of all the open holes. This complementary set is of null measure if the condition (6) holds.

is decreasing and its limiting value vanishes for $j \to \infty$ because of the complete space filling condition (6). A sketch of the iterative process as a Swiss-cheese construction, is shown in figure 2 in the 2D case.

It is clear from the construction shown in figure 2 that the LL algorithm is a variant of the Sierpiński algorithm used to build 3D Menger cubes [19]. Let us recall that, similarly to the asymptotic complete sphere-packing, Menger cubes have asymptotically zero volume (corresponding to (6)) and infinite surface (corresponding to (7)). Noticeable differences are: (1) open spheres (open disks in 2D space) are removed at each rank, instead of open cubes for the Menger sponge; (2) LL algorithm is basically random (though it is not mandatory) whereas Sierpiński algorithm is usually regular.

The only condition (by induction) required for the LL algorithm to be continued to infinity is that $n_j \leqslant \nu_j$ at each rank j. This is an explicit sufficient condition, but hard to use because the intricate shape of void domains complicates the task of calculating the number ν_j of plesiohedra included in the void domain Ω_{j-1}. To overcome this difficulty, one could search analytically for the lower-bound number of plesiohedra, depending on the actual shape of Ω_{j-1}. If such a lower-bound can be found (named R_j), the less stringent sufficient condition $n_j < R_j$ can be used instead for each value of $j = 1, 2, \ldots$.

3.3. Determining R_j

Considering the system at rank $j-1$, the domain Ω_{j-1} is the union of ν_j complete polyhedra $\omega(r_j)$ ('complete polyhedron' means here: 'totally inside Ω_{j-1}') and of a domain $\delta\Omega_j$, of volume δV_j, which is too thin to accept any complete polyhedron $\omega(r_j)$:

$$V_{j-1} = \nu_j v_j + \delta V_j. \tag{10}$$

By construction, the domain $\delta\Omega_j$ cannot include any sphere of diameter $2\gamma_c r_j$ (that is the diameter of the sphere circumscribing a polyhedron $\omega(r_j)$). Then δV_j is smaller than the sum of the volumes of the outer shells of width $2\gamma_c r_j$ around each sphere of rank $k \leqslant j-1$:

$$\delta V_j \leqslant \frac{4\pi}{3}\sum_{k=0}^{j-1} n_k \left[\left(r_k + 2\gamma_c r_j\right)^3 - r_k^3\right]. \tag{11}$$

The inequality (11) is the key ingredient that allows one to write explicitly a sufficient condition for the population (4) of spheres to be space-filling. This inequality is more precise than the corresponding inequality written by LL in their work (the expression (3.4) in [15]) and it results in a much better estimate of the lower bound R_j. Using (6), (9) and (11), the following lower bound for ν_j is obtained:

$$\nu_j \geqslant \frac{3}{4\pi\alpha_v}\frac{1}{r_j^3} - \frac{1}{\alpha_v}\sum_{k=0}^{j-1} n_k \left(\frac{r_k}{r_j} + 2\gamma_c\right)^3. \tag{12}$$

It results in the sufficient condition (named: $(\mathcal{C}S1)$):

The LL algorithm builds a space-filling packing of spheres with distribution (4)–(7) if the inequality:

$$\frac{3}{4\pi}\frac{1}{n_j r_j^3} - \sum_{k=0}^{j-1} \frac{n_k}{n_j}\left(\frac{r_k}{r_j} + 2\gamma_c\right)^3 \geqslant \alpha_v, \tag{13}$$

holds true for every value of $j = 1, 2, \ldots$.

In (13), the parameters α_v and γ_c depend only on the plesiohedron used in the LL algorithm.

4. Sufficient condition for a generic fractal sphere population

In this section we shall derive the sufficient condition on the exponent d_f, for the discrete distribution of spheres (4)–(7) with:

$$n_k = n_0 n^k; \qquad r_k = \frac{r_0}{n^{k/d_f}}, \quad k = 0, 1, 2, \ldots, \infty \tag{14}$$

such that these spheres are space-filling using the LL algorithm. This *discrete* distribution writes as $n_k \propto 1/r_k^{d_f}$, similar to the *continuous* distribution (1) written as: $n(r)\mathrm{d}r = (1/r^{d_f})\mathrm{d}r/r$.

Indeed, from (14), the index k is proportional to the logarithm of the corresponding radius, hence the term $\mathrm{d}r/r$ may be put aside in the continuous distribution.

There are four constant parameters in (14): n_0 and n are two integer numbers such that $n_0 \geqslant 1$ and $n \geqslant 2$, and two real parameters r_0 and d_f such that $0 < r_0 < 1/(2^{5/6} n_0^{1/3})$ and $2 \leqslant d_\mathrm{f} < 3$, to be consistent with (5) and (7). We have also the rough but useful inequality: $\gamma_\mathrm{c} r_0 < 1$, which comes from $r_0 < 1/2$ (because the edge length of the cube is 1), and $\gamma_\mathrm{c} < 2$.

We note first that, using the distribution (14), the space-filling condition (6) writes as the equality:

$$\frac{4\pi}{3} n_0 r_0^3 = 1 - n^{1-3/d_\mathrm{f}}, \tag{15}$$

from which the volume fraction of the system at rank $j \geqslant 0$, namely $\phi_j = \sum_{k=0,\ldots,j} n_k 4\pi r_k^3/3$, is found to depend only on the two parameters n and d_f:

$$\phi_j = 1 - \frac{1}{n^{(j+1)(3/d_\mathrm{f}-1)}}. \tag{16}$$

Since $n \geqslant 2$, ϕ_j tends clearly to 1 when $j \to \infty$. This formula can also be written:

$$1 - \phi_j = \left(\frac{r_{j+1}}{r_0}\right)^{3-d_\mathrm{f}}, \tag{17}$$

a popular formula for the porosity of fractal sphere-packing [36] (in theoretical physics) and of concrete [37] (in applied physics).

4.1. The seed-particle radius r_0

From the equality (15), the condition (5) gives an upper bound of the parameter n:

$$2 \leqslant n < 2^{2d_\mathrm{f}/(3-d_\mathrm{f})}, \tag{18}$$

where we used for the sake of simplicity the inequality: $1 - \pi/\sqrt{18} > 1/4$.

Also from (15), one finds the value of r_0 as a function of the three other parameters n_0, n and d_f:

$$r_0 = \left(\frac{3}{4\pi n_0}\left(1 - n^{1-3/d_\mathrm{f}}\right)\right)^{1/3}. \tag{19}$$

4.2. The condition $R_j/n_j \geqslant 1$

Using (14) and (19), the sufficient condition (13) is written:

$$f_1 + \frac{6\gamma_\mathrm{c}}{n^{j(1-2/d_\mathrm{f})}} g_2 + \frac{12\gamma_\mathrm{c}^2}{n^{j(1-1/d_\mathrm{f})}} g_1 + \frac{8\gamma_\mathrm{c}^3}{n^j} g_0 \geqslant \alpha_\mathrm{v}, \tag{20}$$

in which the four functions f_1, g_0, g_1, g_2, independent of the rank j, are given by:

$$f_1 \equiv \frac{1}{1 - n^{1-3/d_\mathrm{f}}} - \left(\frac{6\gamma_\mathrm{c}}{n^{1-2/d_\mathrm{f}} - 1} + \frac{12\gamma_\mathrm{c}^2}{n^{1-1/d_\mathrm{f}} - 1} + \frac{8\gamma_\mathrm{c}^3}{n - 1}\right), \tag{21}$$

$$g_m \equiv \frac{1}{n^{1-m/d_\mathrm{f}} - 1}, \tag{22}$$

and $m = 0, 1, 2$. Since all the functions g_m are > 0, the relation (20) is fulfilled if the weaker inequality (independent on the rank j): $f_1 > \alpha_\mathrm{v}$ is realized.

4.3. Summarizing the sufficient condition

The corresponding sufficient condition (named: ($\mathcal{CS}2$)) is written as:

The LL algorithm builds a perfect space-filling packing of spheres with the distribution (14) if there is at least one integer number $n \in [2, 2^{2d_\mathrm{f}/(3-d_\mathrm{f})})$ (the notation $[\alpha, b)$ denotes the interval $\alpha \leqslant n < b$), such that:

$$f_1 \equiv \frac{1}{1 - n^{1-3/d_\mathrm{f}}} - \left(\frac{6\gamma_\mathrm{c}}{n^{1-2/d_\mathrm{f}} - 1} + \frac{12\gamma_\mathrm{c}^2}{n^{1-1/d_\mathrm{f}} - 1} + \frac{8\gamma_\mathrm{c}^3}{n - 1} \right) > \alpha_\mathrm{v}. \tag{23}$$

Once the inequality (23) is fulfilled for a value of n, we may select any integer number n_0 such that:

$$n_0 > \frac{6}{\pi} \left(1 - \frac{1}{n^{3/d_\mathrm{f}-1}} \right), \tag{24}$$

which comes from the fact that $r_0 < 1/2$ (no sphere can be larger than the edge length of the box) and relation (15). At last, the value of r_0 is given by (19) as a function of d_f, n and n_0.

5. Explicit sufficient conditions for various space-filling polyhedra approaching the derivation for spheres

5.1. The cube

The cube has parameters:

$$\gamma_\mathrm{c} = \sqrt{3}; \qquad \alpha_\mathrm{v} = \frac{6}{\pi}, \tag{25}$$

hence the expression of the function f_1:

$$f_1 \equiv \frac{1}{1 - n^{1-3/d_\mathrm{f}}} - \left(\frac{6\sqrt{3}}{n^{1-2/d_\mathrm{f}} - 1} + \frac{36}{n^{1-1/d_\mathrm{f}} - 1} + \frac{24\sqrt{3}}{n - 1} \right). \tag{26}$$

The function f_1 is an increasing function of d_f for any fixed value of $n > 2$. The inequation $f_1 \geqslant 6/\pi$, with f_1 given in (26) admits solutions in integer numbers $n \in [2, 2^{2d_\mathrm{f}/(3-d_\mathrm{f})})$ for any value of d_f in the range:

$$2.855 \leqslant d_\mathrm{f} < 3. \tag{27}$$

The evolution of f_1 as a function of n is plotted in figure 3 for several relevant values of d_f.

The sufficient condition (27) is much wider than the set of discrete values $d_\mathrm{f} = 2 + \log p/\log(p+1)$ (with p any integer $\geqslant 26$) derived in [15] and which are all included in the range $[2.9885, 3)$.

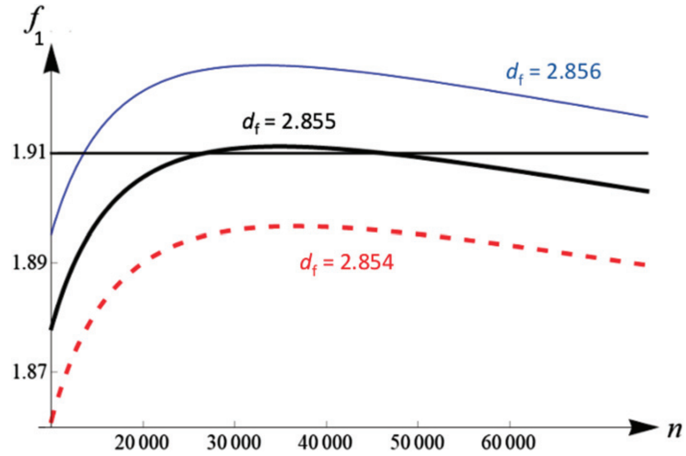

Figure 3. Shape of the function f_1 as given in (26) in the case of the cube as the plesiohedron used in the LL algorithm. Three values of the fractal dimension d_{f} are used to exemplify the threshold of (23). The maximum of the function f_1 increases regularly with the value of d_{f}. For $d_{\mathrm{f}} > 2.855$, the values of f_1 are larger than $\alpha_{\mathrm{v}} = 6/\pi \simeq 1.91$ (the horizontal line) on some interval of *n*, making true the sufficient condition for the sphere population (14) to be space-filling.

5.2. The rhombic dodecahedron

This polyhedron has parameters:

$$\gamma_{\mathrm{c}} = \sqrt{2}; \qquad \alpha_{\mathrm{v}} = 8. \tag{28}$$

It is closer to the sphere in the sense that the value of γ_{c} is smaller than that of the cube. The same analysis as before leads to the sufficient condition:

$$2.847 \leqslant d_{\mathrm{f}} < 3, \tag{29}$$

that is a slightly wider range than for the cube case.

5.3. The truncated octahedron

This polyhedron is more interesting than the previous one since its parameters:

$$\gamma_{\mathrm{c}} = \sqrt{5/3}; \qquad \alpha_{\mathrm{v}} = 8/\pi\sqrt{3}, \tag{30}$$

show that its shape is much closer to the shape of a sphere (the ratio between the radius of the circumscribed sphere and the one of the inscribed sphere is only 1.29). In this case, the same analysis as before leads to the sufficient condition:

$$2.800 \leqslant d_{\mathrm{f}} < 3. \tag{31}$$

The stricter sufficient condition ($\mathcal{CS}1$) allows the replacement of the lower threshold 2.800 by 2.798 in (29).

In short, using the sufficient condition ($\mathcal{CS}2$) with, successively, the cube, the rhombic dodecahedron and the truncated octahedron as the plesiohedra required in the LL algorithm, we showed the following theorem:

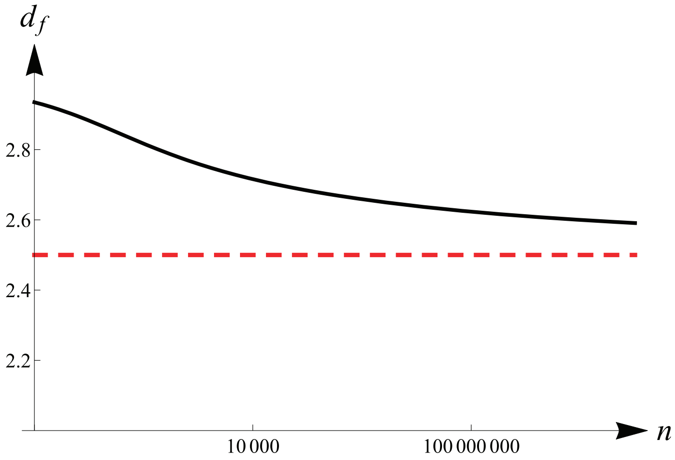

Figure 4. Solution (black curve) in d_f of the equation (33) versus the variable n. The red dashed line is the special value $d_f = 5/2$. The asymptotic solution for $n \to \infty$ is $d_f \simeq 5/(2 - \log 6/\log n) \to 5/2$. This figure shows that, for any given value of d_f, the inequation (32) has solution in n only if $d_f > 5/2$.

- for any value of d_f in the range $2.8 \leqslant d_f < 3$, it is possible to pack iteratively $n_k \propto 1/r_k^{d_f}$ spheres of radii in geometric progression $r_k \propto \rho^k$ (with $0 < \rho < 2^{-1/3}$) in the unit 3D cubic box. The packing is complete in the sense that the packing density equals 1 for $k \to \infty$.

5.4. A note about the best possible sufficient condition

The only parameters of the sufficient condition (23) are γ_c and α_v of the plesiohedron used in the LL algorithm. The more sphere-like is the plesiohedron, and the closer to 1 are these two parameters, no matter how complicated the shape of the polyhedron. Even aperiodic space tiling [38] can be used as well. So far, we have considered only three plesiohedra, with the truncated octahedron having a shape relatively close to the sphere (this is the 'Kelvin's polyhedron' [39]).

At this juncture, one wonders how much more the range of fractal dimensions given by (31) could be expanded, if all possible plesiohedra (known or yet to be discovered) were considered in this gradual geometrical approach towards perfect sphericity. A partial answer may be gleaned from the remark that the parameters $\gamma_c > 1$ and $\alpha_v > 1$ for any plesiohedron, with limiting values $= 1$ for both parameters (these limit values are the respective values for the perfect sphere). Let us then suppose that we know a sequence of different plesiohedra with decreasing values of γ_c approaching 1. Such sequence could begin with:/cube ($\gamma_c = 1.73$)/rhombic dodecahedron ($\gamma_c = 1.35$)/truncated octahedron ($\gamma_c = 1.29$)/.... Provided such a sequence exists, the smallest value of d_f compatible with a space-filling sphere population (14) under the LL algorithm, is given by the sufficient condition (23) written with $\gamma_c = \alpha_v = 1$:

$$\frac{1}{1 - n^{1-3/d_f}} - \left(\frac{6}{n^{1-2/d_f} - 1} + \frac{12}{n^{1-1/d_f} - 1} + \frac{8}{n - 1} \right) > 1. \tag{32}$$

We first solve numerically the corresponding equation in d_f, with the variable $n > 1$:

$$\frac{1}{1 - n^{1-3/d_f}} - \left(\frac{6}{n^{1-2/d_f} - 1} + \frac{12}{n^{1-1/d_f} - 1} + \frac{8}{n - 1} \right) = 1. \tag{33}$$

Table 1. Parameters of a possible numerical simulation of sphere-packing using the LL algorithm with truncated octahedron as the plesiohedron. The sphere population is chosen with fractal dimension $d_\mathrm{f} = 2.875$, $n = 74$ and $n_0 = 2$. When the rank j of the iteration increases, the total number, N_s, of spheres increases exponentially, while the volume fraction ϕ_j increases very smoothly. Numerical simulation of such sphere packing is hardly conceivable beyond the rank $j = 4$ using this method.

j	N_s	r_j	ϕ_j
0	2	0.2731	0.171
1	150	0.0611	0.312
2	11 102	0.0137	0.430
3	821 550	0.003	0.527
4	6.0×10^7	6.8×10^{-4}	0.608
5	4.5×10^9	1.5×10^{-4}	0.675
6	3.3×10^{11}	3.4×10^{-5}	0.730
...	...	...	...
15	2.2×10^{28}	4.8×10^{-11}	0.950
...	...	...	...

For any value of n, there is only one solution of (33), which is shown in the figure 4. Moreover, when $n \gg 1$, the two first terms of (33) are dominant, and the equation leads to:

$$n^{2-5/d_\mathrm{f}} \simeq 6 \tag{34}$$

that is: $d_\mathrm{f} \simeq 5/(2 - \log 6/\log n)$ which tends to $5/2$ when $n \to \infty$.

There is no acceptable solution corresponding to $d_\mathrm{f} \leqslant 5/2$. The more general sufficient condition ($\mathcal{C}S1$) leads to the same conclusion since the left-hand term of (13), calculated for $d_\mathrm{f} = 5/2$, grows from a negative value for $n = 2$, to the value 1^- (as $1–5/n^{1/5}$ when $n \to \infty$) for any value of j.

We conclude that, using the algorithm LL, the range of values of d_f sufficient for the packing of spheres (14) to be space-filling is always included in the interval:

$$5/2 < d_\mathrm{f} < 3.$$

An interesting remark here is that the Apollonian fractal dimension $d_\mathrm{f}^{\mathrm{Apo}} \simeq 2.4739 \pm 0.0010$ being smaller than 2.5, the Apollonian sphere-packing *cannot* be a population (14) packed using the LL algorithm, whatever the plesiohedron we use in this algorithm. In section 6, we will examine more closely the difference between packings resulting from LL and from Apollonian constructions.

5.5. Conceivable improvements of the theorem

As discussed in section 5.4, the theorem derived in section 5.3 can be straightforwardly improved using space-filling polyhedra 'rounder' than the truncated octahedron adhering to the sufficient condition (23). These polyhedra remain to be found, and their values of α_v and γ_c can then be calculated to see how the range of acceptable d_f is affected.

A more complicated improvement might result from finding a better lower bound R_j of the coefficients ν_j, following the reasoning detailed in section 3.3. This would require an analysis of the shapes of the voids left in the intermediary sphere packings, more carefully than the simple calculation presented in section 3.3. This approach could probably be effective, but requires much work.

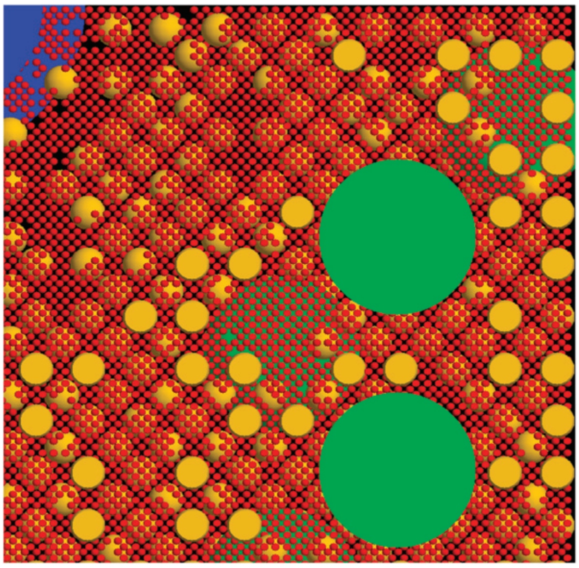

Figure 5. Cut-through of a rank 3 sphere-packing obtained using the LL algorithm with truncated octahedra as the generic plesiohedron. The parameters are: $d_f = 2.875$, $n = 74$, $n_0 = 2$. Colours correspond to the sizes of the spheres (that is: $r_0 = 0.273$ (blue), $r_1 = 0.061$ (green), $r_2 = 0.014$ (yellow), $r_3 = 0.003$ (red)). The figure shown represents 10% of the unit cube. Since it is a 2D projection of a 3D arrangement of spheres, this image is not as informative as the 2D model shown in figure 2. However, one can see clearly the underlying regular truncated-octahedra honeycomb used by the LL algorithm, despite the random selection of the sphere locations amongst the available sites at each iteration.

Another improvement consistent with the LL algorithm would include tessellation of space with two (or more) different sorts of polyhedra [40]. This would change the formula appearing in the sufficient condition ($\mathcal{C}S1$), involving then two (or more) values of γ_c and α_v. That way, two (or more) sphere radii in fixed ratios between them would have to be considered at each rank of the LL algorithm iteration.

6. A numerical example

In this section, we propose using the LL algorithm to build numerically the first stages of a sphere packing in the cube of edge-length $L = 1$ with periodic boundary conditions. The fractal dimension $d_f = 2.875 > 2.8$ is selected, and we use the truncated octahedron in the algorithm.

The inequation (23) solves as:

$$74 \leqslant n \leqslant 2.210^{11}. \tag{35}$$

Selecting the value $n = 74$ and the number $n_0 = 2$ of initial spheres, we give in table 1 the characteristics of the numerical simulation compatible with the parameters deduced from the sufficient condition (23).

We performed a numerical simulation up to $j = 3$ (number total of spheres: $N_s = 821\,550$) using the LL algorithm starting from 2 randomly-placed spheres of radius $r_0 = 0.2731$ in the

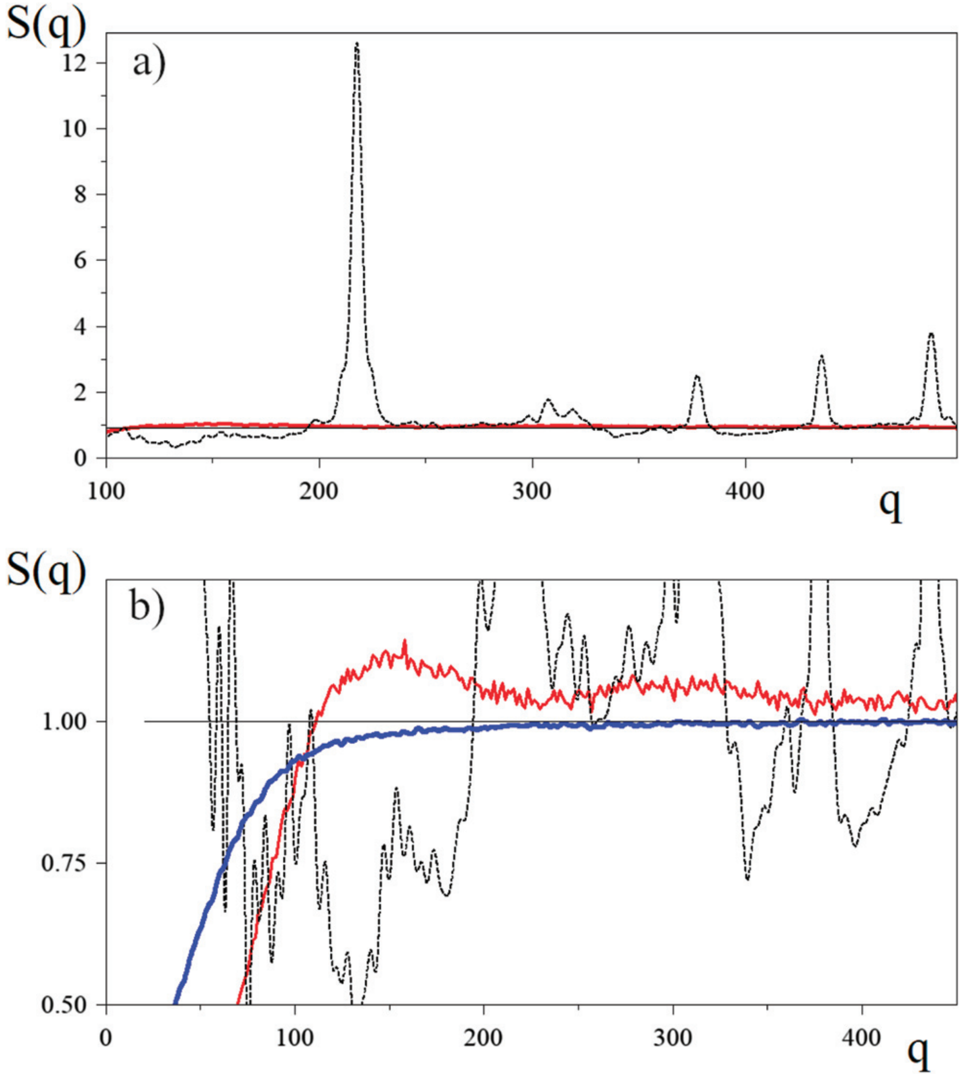

Figure 6. (a) Dotted black curve: structure factor of the packing of spheres shown in figure 5, built using the LL algorithm up to third rank (system of 821 550 spheres averaged over space orientations). The restricted Bragg peaks are due to the limited crystallite sets inherent to the LL algorithm. The unit of the variable q is determined by the choice of the unit length (the edge of the cube), and the range of $S(q)$ values if chosen for the first Bragg peak be shown in full. Red curve: structure factor of an Apollonian packing (system of 800 000 spheres averaged over space orientations), as discussed in [17]. Bragg peaks are absent from the Apollonian packing structure factor; (b) magnification of the values of the structure factors shown in figure (a). Dotted black curve: LL sphere packing; red curve: Apollonian sphere packing. The structure factor of a packing structure obtained using Manna's algorithm is shown for comparison (blue curve; system of 800 000 spheres averaged over space orientations). No Bragg peak is seen either in the Apollonian packing or in the Manna packing structure factor. On the other hand, Manna packing is seen to be much less correlated (no peak visible) than Apollonian packing (shallow peaks), due to the release of the extremality condition of the Apollonian algorithm (namely: every particle to add tries to fill the *largest void* in the structure).

unit cube. At every rank $k = 1, 2, 3$, the selection of the n_k truncated octahedra among the ν_k, is performed randomly. Visualization of a small part of the packing showing the particles of ranks 0, 1, 2 and 3 is shown in figure 5, and the successive regular lattices, on which the truncated octahedra are lying, are quite visible on it.

A similar conclusion about the spurious evidence of local lattices of plesiohedra in the LL algorithm case can be drawn from the analysis of the sphere-packing in the reciprocal space. The reciprocal space is the natural framework to analyze the Small-Angle X-ray Scattering data from systems of particles. In this space, the natural coordinate frame is represented by the scattering wave vector coordinate $\mathbf{q} = (2\pi/\lambda)(\mathbf{u}_{\mathrm{sca}} - \mathbf{u}_{\mathrm{inc}})$, in which λ is the wavelength of the scattered X-ray, and $\mathbf{u}_{\mathrm{inc}}, \mathbf{u}_{\mathrm{sca}}$ are the unit vectors in the incident and scattered directions respectively. The static structure factor [41]:

$$S(\mathbf{q}) = \sum_{i,j} f_i f_j \, \mathrm{e}^{\mathbf{i}\mathbf{q}(\mathbf{r}_i - \mathbf{r}_j)} \Big/ \sum_i f_i^2, \tag{36}$$

of an ensemble of spheres (the centre of the sphere labelled i is located at $\mathbf{r}_i$, and its form factor is f_i) is a measured quantity which includes most of the information about the spatial arrangement of the spheres in the system. The structure factor depends only on the modulus $q = 4\pi/\lambda \sin(\theta/2)$, in which θ is the scattering angle, when spherical symmetry applies.

In the case of the LL algorithm packing of spheres, the structure factor function remains close to the value 1, except a number of strong fine peaks reminiscent of Bragg peaks coming from the bcc symmetry of the tessellation of space by truncated octahedra (see dotted black curves in figure 6). The LL structure factor is quite different from the structure factor of an Apollonian packing (red curves) and from the structure factor of a Manna packing (blue curve on figure 6(b)). This result confirms our conjecture that the osculatory algorithms are different in essence from the LL algorithm, regardless of the value of the fractal dimension ($d_{\mathrm{f}} \simeq 2.47$ for the Apollonian packing; $d_{\mathrm{f}} \simeq 2.73$ for the Manna packing).

7. Conclusion

In the present work, we extended a theorem from LL to derive a wide range of values of the exponent d_{f} for which a population of spheres with continuous radius-distribution $\sim 1/r^{d_{\mathrm{f}}+1}$ is space-filling. The method can probably be improved and hints are given in the text. Although the basis of the LL algorithm does not allow for the inclusion of all possible space-filling populations of spheres—as evidenced by the comparison with Apollonian packing—the extended LL theorem nevertheless grants access to a much larger set of sphere populations, previously unknown or unexplored.

Physical properties of extremely dense sphere packings, as generated by the LL algorithm or by the Apollonian osculatory algorithm, remain to be discovered. However, unusual properties can be expected if one refers to the case of the Menger sponges since both sorts of systems share basic features (e.g. extreme density, extreme surface, self-similar spatial distribution of matter, etc). Indeed, Menger sponges are known for the spectacular—and still unexplained—localization of electromagnetic waves [42] or strongly anomalous thermal diffusion [43]. But unlike the Menger cubes—which are artificial structures—, extremely dense sphere packings appear naturally as high internal-phase-ratio emulsions [8, 17]. For studies and applications involving physical properties of extreme sphere-packing, the role of the exponent d_{f} is probably of utmost importance and we may now begin to understand how the value of d_{f} is related to the building process.

Data availability statement

The data that support the findings of this study are available upon reasonable request from the authors.

ORCID iDs

Robert Botet https://orcid.org/0000-0002-8515-111X
Sylvie Kwok https://orcid.org/0000-0001-8261-5807
Bernard Cabane https://orcid.org/0000-0002-5366-7592

References

[1] Edington J W, Melton K N and Cutler C P 1976 *Prog. Mater. Sci.* **21** 61–170
[2] Kobwittaya K and Watari T 2019 *Materials Chemistry of Ceramics* ed J Hojo (Berlin: Springer) pp 181–211
[3] Wachtman J B (ed) 1969 *Mechanical and Thermal Properties of Ceramics* vol 303 (Washington D.C.: NBS Special Publication)
[4] Smirnov A V, Ponomarev S G, Tarasovskii V P, Rybal'chenko V V, Vasin A A and Belov V V 2019 *Glass Ceram.* **75** 345–51
[5] Schmidt M, Fehling E and Geisenhanslüke C (ed) 2004 *Ultra High Performance Concrete (UHPC) - Proc. of the Int. Symp. on Ultra High Performance Concrete* (Kassel, Germany 13–15 September 2004) (Kassel University Press GmbH)
[6] Lange F F 1989 *J. Am. Ceram. Soc.* **72** 3–15
[7] Darcovich K, Béra L and Shinagawa K 2003 *Mater. Sci. Eng.* A **341** 247–55
[8] Kwok S, Botet R, Shglabow A and Cabane B 2020 *Europhys. Lett.* **130** 38001
[9] Gardner M 2001 *The Colossal Book of Mathematics: Classic Puzzles. Paradoxes, and Problems* vol 135 (New York: Norton)
[10] Conway J H and Torquato S 2006 *Proc. Natl Acad. Sci.* **103** 10612–7
[11] Torquato S and Jiao Y 2009 *Phys. Rev.* E **80** 041104
[12] Borkovec M, de Paris W and Peikert R 1994 *Fractals* **02** 521–6
[13] Dodds P S and Weitz J S 2002 *Phys. Rev.* E **65** 056108
[14] Stäger D V and Herrmann H J 2018 *Fractals* **26** 1850022
[15] Lieb E H and Lebowitz J L 1972 *Adv. Math.* **9** 316–98
[16] Hartmann W K 1969 *Icarus* **10** 201–13
Pettijohn F J 1957 *Sedimentary Rocks* (New York: Harper and Brothers)
[17] Kwok S, Botet R, Sharpnack L and Cabane B 2020 *Soft Matter* **16** 2426–30
[18] Leibniz G W 2007 *The Leibniz-Des Bosses Correspondence* ed B Look and D Rutherford (New Haven, CT: Yale University Press)
[19] Mandelbrot B B 1983 *The Fractal Geometry of Nature* (San Francisco, CA: Freeman)
[20] Farr R S and Griffiths E 2010 *Phys. Rev.* E **81** 061403
[21] Varratto F and Foffi G 2011 *Mol. Phys.* **109** 2663–9
[22] Melzac Z A 1966 *Can. J. Math.* **18** 838–52
[23] Manna S S 1992 *Physica* A **187** 373–7
[24] Jaeger H M and Nagel S R 1992 *Science* **255** 1523–31
[25] Kontorovich A, Oh H and Shah N 2011 *J. Am. Math. Soc.* **24** 603
[26] Aste T 1996 *Phys. Rev.* E **53** 2571
[27] Tricot C 1984 *Math. Proc. Camb. Phil. Soc.* **96** 413423
[28] Boyd D W 1973 *Mathematika* **20** 170–4
[29] Amirjanov A and Sobolev K 2006 *Modelling Simul. Mater. Sci. Eng.* **14** 789–98
[30] Wesler O 1960 *Proc. Am. Math. Soc.* **11** 324
The theorem was proved in this article for complete filling of the unit sphere by polydisperse spheres, but it can be demonstrated the same way for the complete filling of the unit cube.
[31] Sahu K K and Lahiri A K 2004 *Phil. Mag.* **84** 1185–96

[32] Hilbert D and Cohn-Vossen S 1999 *Geometry and the Imagination* (New York: AMS Chelsea)
[33] Sorabji R (ed) 2009 *Simplicius, On Aristotle: On the Heavens 3.7–4.6* (London: Bloomsbury)
[34] Grünbaum B and Shephard G C 1980 *Bull. Am. Math. Soc* **3** 951–73
[35] Omnés R 1985 *J. Physique* **46** 139–47
[36] Herrmann H J, Mantica G and Bessis D 1990 *Phys. Rev. Lett.* **65** 3223–6
[37] Caquot M A 1937 *Le role des matériaux inertes dans le béton in Société des Ingénieurs Civils de France* vol 4 (Paris: Hôtel de la Société) pp 563–82
[38] Grünbaum B and Shephard G C 1980 *Tilings and Patterns* (San Francisco, CA: Freeman) ch 10
[39] Weaire D 1996 *The Kelvin Problem: Foam Structures of Minimal Surface Area* (London: Taylor and Francis)
[40] Conway J H, Jiao Y and Torquato S 2011 *Proc. Natl Acad. Sci.* **108** 11009–12
[41] Sorensen C M 2001 *Aerosol Sci. Technol.* **35** 648–87
[42] Miyamoto Y, Kirihara S, Takeda M W, Honda K and Sakoda K 2005 *Advances in Ceramic Coatings and Ceramic-Metal Systems* (*Ceramic Engineering and Science Proceedings* vol 26) ed D Zu and K Plucknett (Westerville: The American Ceramic Society) pp 349–60
[43] Herrmann R 2015 *Chaos Solitons Fractals* **70** 38–41